Pharmacoscript

Aji et al./Pharmacoscript, Volume 9, No, 1, Februari 2026, 234-258

P-ISSN : 2622-4941 | E-ISSN : 2685-1121

THE POTENTIAL OF TURMERIC RHIZOME EXTRACT AS ANTIBIOFILM AGAINST *Staphylococcus aureus* THROUGH IN SILICO AND IN VITRO APPROACHES

Nur Aji*, Risnawati, Naufal Maulana Rahmaan, Nadine Elysia Tabina

[1]Department of Pharmacy, Poltekkes Kemenkes Tasikmalaya, Tasikmalaya Indonesia

*Email: nuraji090689@gmail.com

Received: 09/02/2026 Revised: 16/03/2026 Accepted: 19/03/2026 Published: 02/04/2026

ABSTRACT

Escalating antibiotic resistance in *Staphylococcus aureus* is driven by biofilm formation, which undermines the efficacy of antibiotics. This study evaluated curcumin from turmeric (*Curcuma longa* L.) as a natural antibiofilm agent using *in silico* and *in vitro* methods. Molecular docking and toxicity predictions were used to test curcumin's interaction with *S. aureus* biofilm proteins. I*n vitro* efficacy was measured by disc diffusion and crystal violet staining assays. *In silico* analysis identified LuxS (PDB ID: 5V2W) as a viable target. Docking validation yielded an RMSD of 3.00 Å and identified 10 potential ligands, including curcumin, auratiamide, and chlorogenic acid. Phytochemical profiling showed that the ethyl acetate fraction had the highest curcuminoid content (24.88% w/w), higher than the 70% ethanol extract (21.69% w/w) and the methanol fraction (0.83% w/w). The ethyl acetate fraction showed moderate antibacterial activity but the strongest antibiofilm effects, with a minimum biofilm inhibitory concentration (MBIC) of 0.05% and an IC_{50} of 0.01%. In conclusion, the ethyl acetate fraction of turmeric enriched with curcuminoids shows strong potential as a natural antibiofilm agent. Computational and experimental evidence support this. These findings suggest the fraction is a promising candidate for topical antibiofilm development. Future research should focus on formulating this fraction in topical delivery systems and testing its efficacy in *ex vivo* skin or dermal infection models to assess clinical potential.

Keywords: Biofilm, In Silico, In Vitro, *Staphylococcus aureus,* Turmeric

INTRODUCTION

Acne vulgaris is a chronic inflammatory skin disease of the pilosebaceous unit with a global prevalence of 9.38%, high in Southeast Asia (40–80%) and Indonesia, especially in adolescents (80–85%) and some adults (12% of women >25 years) (Heng & Chew, 2020). The causes are multifactorial, including increased sebum, follicular hyperkeratinization, colonization by *Cutibacterium acnes* and *Staphylococcus aureus*, and immune responses, which not only cause physical symptoms but also psychological impacts such as decreased self-confidence and depression (Anindyaguna et al., 2025). Treatment for

mild to moderate acne generally uses topical agents (retinoids, benzoyl peroxide, azelaic acid, antibiotics), while moderate to severe cases require oral antibiotics or isotretinoin (Reynolds et al., 2024). However, long-term antibiotic use without a combination of non-antibiotic agents can lead to resistance in *C. acnes*, *S. epidermidis*, and *S. aureus* (Legiawati et al., 2023).

Antibiotic resistance in *C. acnes*, *S. epidermidis*, and *S. aureus* arises from genetic adaptation and selective pressure. *S. aureus* represents a major concern, with global macrolide resistance reported at 57.3% (Navidifar et al., 2025). In Indonesia, *S. aureus* has been found in acne lesions with a resistance pattern similar to that of *C. acnes*, acting as a reservoir of resistance through mecA and biofilms, making it more tolerant to antibiotics and contributing to therapy failure (Gehrke et al., 2023).

Biofilms form extracellular polymeric substances (EPS) that inhibit antibiotic penetration, suppress bacterial metabolism, and are controlled by quorum-sensing mechanisms that activate EPS genes and various virulence factors. In *S. aureus*, in addition to the Agr system, cell communication also involves an autoinducer-2 (AI-2)-based system mediated by the LuxS protein. The LuxS protein was selected as a target because it plays a role in AI-2 production, which regulates bacterial communication and contributes to biofilm formation (Chen et al., 2020). Therefore, new therapeutic strategies focus on inhibiting biofilm formation through quorum quenching and on using antibiofilm plant extracts to enhance acne treatment efficacy.

Turmeric (*Curcuma longa*) contains curcumin, a bioactive compound with well-known antibacterial properties and the potential to inhibit *S. aureus* biofilm formation. This activity may be further supported by other phytochemicals present in turmeric, such as phenols, flavonoids, and tannins (Kashi et al., 2024). Given that biofilm formation plays a crucial role in increasing bacterial tolerance to antibiotics, the discovery of antibiofilm agents requires approaches that efficiently identify active compounds and elucidate their potential mechanisms of action.

In this context, integrating in silico and in vitro approaches has become an effective strategy, in which in silico molecular docking enables rapid screening and interaction prediction between bioactive compounds and molecular targets involved in biofilm regulation, while in vitro assays are necessary to experimentally validate the predicted antibiofilm activity. This combined approach not only accelerates the identification of promising candidates but

also reduces the risk of false-positive predictions from computational screening. Therefore, the increasing problem of antibiotic resistance in acne vulgaris has encouraged the exploration of curcumin from turmeric (*C. longa*) as a potential antibiofilm agent, investigated through integrated in silico and in vitro analyses. This research aims to determine the potential and effectiveness of turmeric (*C. longa*) in inhibiting the formation of *S. aureus* biofilms, as an innovative approach to addressing bacterial resistance that causes acne vulgaris, using in silico and in vitro approaches.

MATERIALS AND METHODS

Materials

S. aureus (ATCC 6538P PK/S), Nutrient Agar (Oxoid), Brain Heart Infusion Broth (Oxoid), turmeric extract, curcumin, 99% DMSO, tetracycline (Oxoid), methanol (Emsure), n-hexane (DPH), ethanol (DPH), ethyl acetate (DPH), blank discs (macherey-Nagel), and phytochemical screening reagents (Dragendorff, Mayers, $FeCl_3$ 1%, gelatin 1%, NaCl 10%, H_2SO_4, acetic acid anhydrous, chloroform, 1% ammonia, and 2N HCl).

Tools

Notebook (130-15IKB), ChemOffice, Molegro Virtual Docker, 48-well microplate (Biologix), micropipettes (Joan Lab), autoclave (ALP), biological safety cabinet (Biobase), incubator (Memmert), rotary evaporator (D-Lab), spectrophotometer (Agilent Cary 60), and standard laboratory glassware.

Method

1. Protein selection and Ramachandran analysis

The molecular docking procedure was initiated by assessing protein quality using the Ramachandran Plot generated through PDBsum (http://www.ebi.ac.uk/thornton-srv/databases/pdbsum/). The phi (φ) and psi (Ψ) angles were plotted on the x- and y-axes, respectively, and the stereochemical quality of the protein model was evaluated based on the distribution of amino acid residues within the *most favoured* and *disallowed regions*.

2. Preparation of Test Ligands

A total of 66 compounds reported in the literature as phytochemical constituents of turmeric were selected as test ligands. Their three-dimensional structures were retrieved from PubChem (https://pubchem.ncbi.nlm.nih.gov) in SDF format using either IUPAC or trivial names and subsequently converted into PDB format for further analysis.

3. Docking Validation and Molecular docking

Docking validation was conducted by re-docking the native ligand into the LuxS protein structure (PDB ID: 5V2W). The robustness of the docking protocol was assessed by calculating the root mean square deviation (RMSD) between the predicted binding pose and the crystallographic conformation. An RMSD value of ≤ 2.0 Å was considered indicative of a reliable protocol. As reported by Warren et al. (2006), RMSD values ≤ 2.0 Å reflect high accuracy, whereas values within the range of 2.0–4.0 Å are still regarded as acceptable for docking validation.

After validation in Molegro Virtual Docker (MVD), docking was performed for the test ligands and positive control ligands against the LuxS receptor. The docking results were evaluated based on the lowest rerank scores. Ligand–receptor interactions were analyzed using the Ligand Map in MVD, and the involved amino acid residues were compared with those of the control ligand, focusing on hydrogen bonds, steric interactions, and electrostatic interactions.

4. Lipinski Analysis and Toxicity

The physicochemical properties of ligands were evaluated based on Lipinski's Rule of Five, including molecular weight (<500 Da), hydrogen bond donors (≤5), hydrogen bond acceptors (≤10), and log P (≤5). Compound names were entered into the Lipinski server (http://www.scfbio-iitd.res.in/software/drugdesign/lipinski.jsp) for analysis. Toxicity prediction, including skin sensitization and Ames test, was performed using pkCSM (https://biosig.lab.uq.edu.au/pkcsm/) after converting compound structures into SMILES format with the SMILES translator (https://cactus.nci.nih.gov/translate/).

5. Fractionation of Turmeric Extract

The concentrated turmeric extract was subjected to liquid–liquid partitioning using a separatory funnel. Initially, the extract was partitioned with n-hexane and water (1:1, v/v). The n-hexane phase was separated and subsequently repartitioned with n-hexane–methanol (1:1, v/v) to yield an n-hexane fraction and a methanol fraction. The aqueous phase obtained from the first step was further partitioned with ethyl acetate–water (1:1, v/v), resulting in an ethyl acetate fraction and a residual aqueous fraction. All organic and aqueous fractions were concentrated under reduced pressure using a rotary evaporator and stored at 4 °C until further analysis (Aji et al., 2022).

6. Turmeric Analysis

The extract used was a 70% ethanol extract of turmeric, obtained from a previous study Armilda et al. (2022), which was

subsequently subjected to liquid–liquid fractionation to obtain n-hexane, ethyl acetate, methanol, and aqueous fractions. The quality of the extract and fraction was confirmed through phytochemical screening and determination of total curcuminoid content. Phytochemical screening was performed for alkaloids, flavonoids, polyphenols, tannins, saponins, triterpenoids, and steroids following the procedure of Farnsworth (1966). The total curcuminoid content was quantified according to the Indonesian Herbal Pharmacopoeia (2008).

a. Alkaloids: The 0,1 g sample was basified with 28% ammonia, partitioned with chloroform, and the chloroform phase was acidified with 2 N HCl. The acid layer was tested with Mayer's reagent (white precipitate) and Dragendorff's reagent (brownish-red precipitate) to indicate the presence of alkaloids.
b. Tannins: The 0,1 g sample was diluted with water and divided into two portions. The first was treated with 1% $FeCl_3$, where blue/blue-black indicated gallotannins or ellagitannins, and green/turquoise indicated condensed tannins. The second was treated with 1% gelatin in 10% NaCl, where precipitate formation indicated tannins.
c. Polyphenols: The 0,1 g sample was diluted with water and treated with 1% $FeCl_3$; the formation of blue, blue-black, green, or turquoise colors indicated polyphenolic compounds.
d. Flavonoids: The 0,1 g sample was dissolved in 80% ethanol, filtered, and the filtrate treated with magnesium powder and concentrated HCl. The formation of orange to red coloration, extractable with amyl or octyl alcohol, indicated flavonoids.
e. Saponins: The 0,1 g sample was diluted with water and shaken vigorously. Stable foam ≥3 cm persisting for 30 minutes indicated saponins.
f. Steroids and triterpenoids: The 0,1 g sample was partitioned with chloroform, the chloroform phase evaporated, and the residue treated with acetic anhydride and concentrated H_2SO_4 (Liebermann–Burchard test). A greenish-blue color indicated steroids, while magenta or violet indicated triterpenoids.
g. Antraquinones: A total of 0,1 g of thick extract was weighed, dissolved in 3 mL of water, and filtered. Subsequently, 1 mL of benzene was added and the benzene layer was collected. The layer was then treated with 2 mL of ammonia

or 0.5 N KOH and shaken. A positive result was indicated by the appearance of a red color in the alkaline layer.

Total curcuminoid content was determined according to the Indonesian Herbal Pharmacopoeia (2008). Approximately 100 mg of turmeric extract/fraction was dissolved in ethanol, filtered, and adjusted to volume. For the reference solution, approximately 10 mg of curcumin standard was accurately weighed and transferred into a 10 mL volumetric flask, then diluted with ethanol to the mark to obtain a stock solution (1000 µg/mL). A series of working standard solutions with concentrations of 2, 4, 6, 8 and 10 µg/mL were prepared from this stock solution. The calibration curve was constructed using these curcumin standards in ethanol, and the absorbance was measured at 425 nm using a UV–Vis spectrophotometer (Figure 1). Sample absorbance was measured under the same conditions, and the total curcuminoid content was calculated from the calibration curve and expressed as % w/w curcumin. All analyses were performed in triplicate.

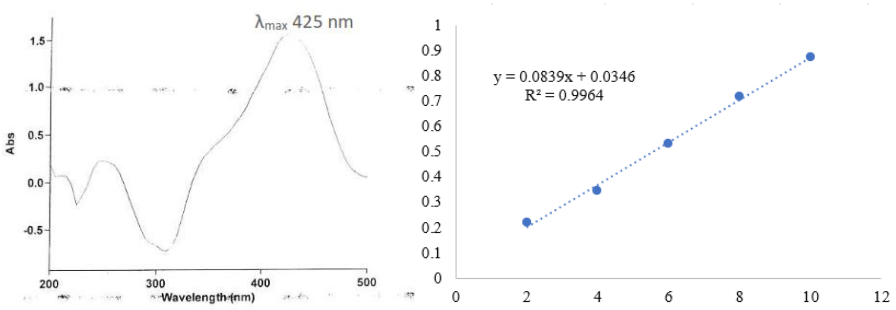

(a) (b)

Figure 1. (a) Wavelength yielded 425 nm for curcumin, and (b) The curcumin calibration curve

7. Antibacterial Activity Test

The antibacterial activity was evaluated using the disc diffusion method against *S. aureus*. A suspension of *S. aureus* was prepared and adjusted to a turbidity standard of 0.5 McFarland, which is equivalent to approximately 1.5×10^8 CFU/mL, and then used as the inoculum for Nutrient Agar (NA) medium. Nutrient Agar was prepared by dissolving 28 g of NA in 1000 mL of distilled water, heated until completely dissolved, and sterilized at 121 °C for 15 minutes. The bacterial inoculum was evenly spread on the surface of NA plates using a sterile cotton swab and allowed to stand for 10–15 minutes. Sterile blank discs were impregnated with 20 µL of the extract and placed on the surface of the inoculated agar using sterile forceps. The plates were incubated at 37 °C for 24 hours,

after which the inhibition zones were observed and measured (Winato et al., 2019).

8. Test the Biofilm Formation Ability of S. aureus

Bacterial cultures were rejuvenated for 24 h and diluted with sterile 0.9% NaCl until turbidity matched the 0.5 McFarland standard. The prepared suspension of *S. aureus* was inoculated into Brain Heart Infusion Broth (BHIB) supplemented with 5% glucose and incubated at 37 °C for 48 h.

9. Antibiofilm Activity Assay

The antibiofilm activity of *S. aureus* was assessed using sterile 48-well microplates. Ethyl acetate fraction was prepared as a stock solution, with DMSO as blank and 0.1% tetracycline HCl as positive control. Bacterial suspension standardized to 0.5 McFarland was mixed with the test samples and BHIB supplemented with 5% glucose, followed by anaerobic incubation at 37 °C for 48 h. After incubation, the medium was discarded, and the wells were rinsed with methanol, then stained with 0.1% crystal violet for 15 min. Excess dye was removed with methanol washing, and plates were dried at 40 °C for 30 min. Bound dye was solubilized with 30% acetic acid for 15 min, and absorbance was measured at 590 nm using a microplate reader to calculate biofilm inhibition percentage (Ibrahim et al., 2020).

10. Biofilm Quantification and IC_{50} Determination

Biofilm formation was quantified based on the optical density (OD_{590}) of bound crystal violet at 590 nm. The percentage of biofilm inhibition formula:

$$\%\ Inhibition = \frac{OD\ blank - ODsample}{OD\ blank}$$

The IC_{50} value, defined as the concentration of fraction causing 50% inhibition of biofilm formation, was determined using linear regression analysis with sample concentration as the x-axis and inhibition percentage as the y-axis. The IC_{50} was calculated using the equation x=(50−b)/a, where *a* is the slope and *b* is the intercept of the regression line (Besan et al., 2023).

RESULT AND DISCUSSION

1. Protein Selection and Ramachandran Analysis

The three-dimensional structure of the LuxS protein (PDB ID: 5V2W) was obtained from the Protein Data Bank (PDB) and prepared prior to molecular docking analysis using Molegro Virtual Docker (MVD). During the preparation process, co-crystallized ligands and water molecules were removed, followed by the addition of missing hydrogen atoms and correction of bond orders and atomic charges to ensure

structural stability of the receptor (Abdullahi et al., 2024). The prepared protein structure was subsequently optimized and inspected to confirm proper geometry, and the potential binding sites were identified using the cavity detection algorithm integrated in MVD to determine the active site for docking simulations. Evaluation of the LuxS protein structure using the Ramachandran plot (Figure 2) showed that 88.4% of residues were located in the most favored regions, 11.0% in additionally allowed regions, and 0.7% in generously allowed regions, with no residues in disallowed regions. The model consisted of 301 non-glycine and non-proline residues, 18 glycine residues, and 16 proline residues, totaling 339 residues. The high proportion of residues in the favored regions indicates that most φ (phi) and ψ (psi) torsion angles adopt sterically and energetically optimal conformations. The absence of residues in disallowed regions further confirms the lack of significant steric clashes, reflecting excellent stereochemical quality. These results validate the structural integrity of the protein model, supporting its reliability for subsequent molecular interaction analysis and structure-based ligand design (Hanifitri et al., 2023).

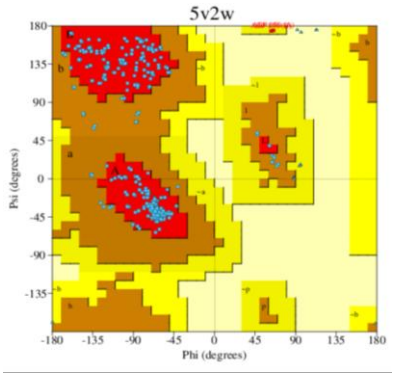

		No. of residues	%-tage
Most favoured regions	[A,B,L]	266	88.4%*
Additional allowed regions	[a,b,l,p]	33	11.0%
Generously allowed regions	[~a,~b,~l,~p]	2	0.7%
Disallowed regions	[XX]	0	0.0%
Non-glycine and non-proline residues		301	100.0%
End-residues (excl. Gly and Pro)		4	
Glycine residues		18	
Proline residues		16	
Total number of residues		339	

Figure 2. Ramachandran analysis of protein suitability

2. Docking Validation

Docking validation was performed by redocking the native ligand into the LuxS protein (PDB ID: 5V2W) (Figure 3), with method reliability evaluated using the RMSD (Root Mean Square Deviation) between the predicted and experimental ligand poses. Lower RMSD values indicate higher accuracy of the predicted binding conformation relative to the native ligand. The validation yielded an RMSD of 3.00 Å, which is within the acceptable range for docking accuracy. According to Warren et al. (2006), RMSD values ≤ 2.0 Å are considered highly reliable, while values between 2.0–4.0 Å remain acceptable for docking validation.

Thus, the obtained RMSD supports the adequacy of the docking protocol for further molecular interaction studies.

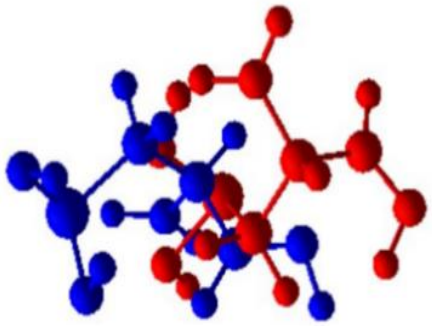

Figure 3. The validation results of the docking of the native ligand Cysteine with CSD_83 [A] show the position before validation (red) and after validation (blue) in the protein cavity region.

3. Docking, Lipinski Analysis and Toxicity Results

Docking analysis of 66 compounds identified 10 ligands with the most favorable binding affinities (Figure 4), including curcumin, auratiamide, chlorogenic acid, rutin, 1,7-bis(3,4-dihydroxyphenyl)-4-hepten-3-one, 1,7-bis(4-hydroxyphenyl), campesterol, 9-hydroxy-10,12,15, 1,3-benzenedicarboxylic acid bis(2-ethylhexyl) ester, and didemethoxybisabolocurcumin. Among these, curcumin demonstrated the most promising interaction profile, consistent with its high curcuminoid content in the ethyl acetate fraction of turmeric. The docking simulations performed with Molegro Virtual Docker utilized the Rerank Score (RS) as the primary indicator, which integrates electrostatic forces, hydrogen bonding, Van der Waals interactions, and torsional strain through the MolDock SE algorithm. Lower (more negative) RS values reflect stronger and more stable ligand–receptor interactions. These results highlight curcumin as the leading candidate, while also suggesting additional bioactive ligands that may contribute synergistically to the antibiofilm potential of turmeric.

In this study, cysteine, the native ligand of LuxS (PDB ID: 5V2W), was used as a reference for docking validation. Cysteine plays a key role in the biosynthesis of autoinducer-2 (AI-2) as part of the pathway involved in the production of 4,5-dihydroxy-2,3-pentanedione (DPD), the precursor of AI-2, and is also linked to methionine metabolism. As shown in Figure 5 and Table 1, cysteine interacts with several key

residues, including Thr130, Arg39, Thr85, Gly82, Arg84, and Gly129, through amino (–NH_2), thiol (–SH), carbonyl (–C=O), and hydroxyl (–OH) groups, which represent important pharmacophoric features. Test ligands that formed interactions similar to the native ligand, particularly through hydrogen bonding and comparable amino acid residues, demonstrated high binding affinity and orientation suitability. Auratiamide, chlorogenic acid, and rutin exhibited the greatest overlap with the native ligand in terms of binding interactions, supported by functional groups such as hydroxyl (–OH), carbonyl (–C=O), carboxyl (–COOH), and amino (–NH_2) (specific to auratiamide) that may act as pharmacophores.

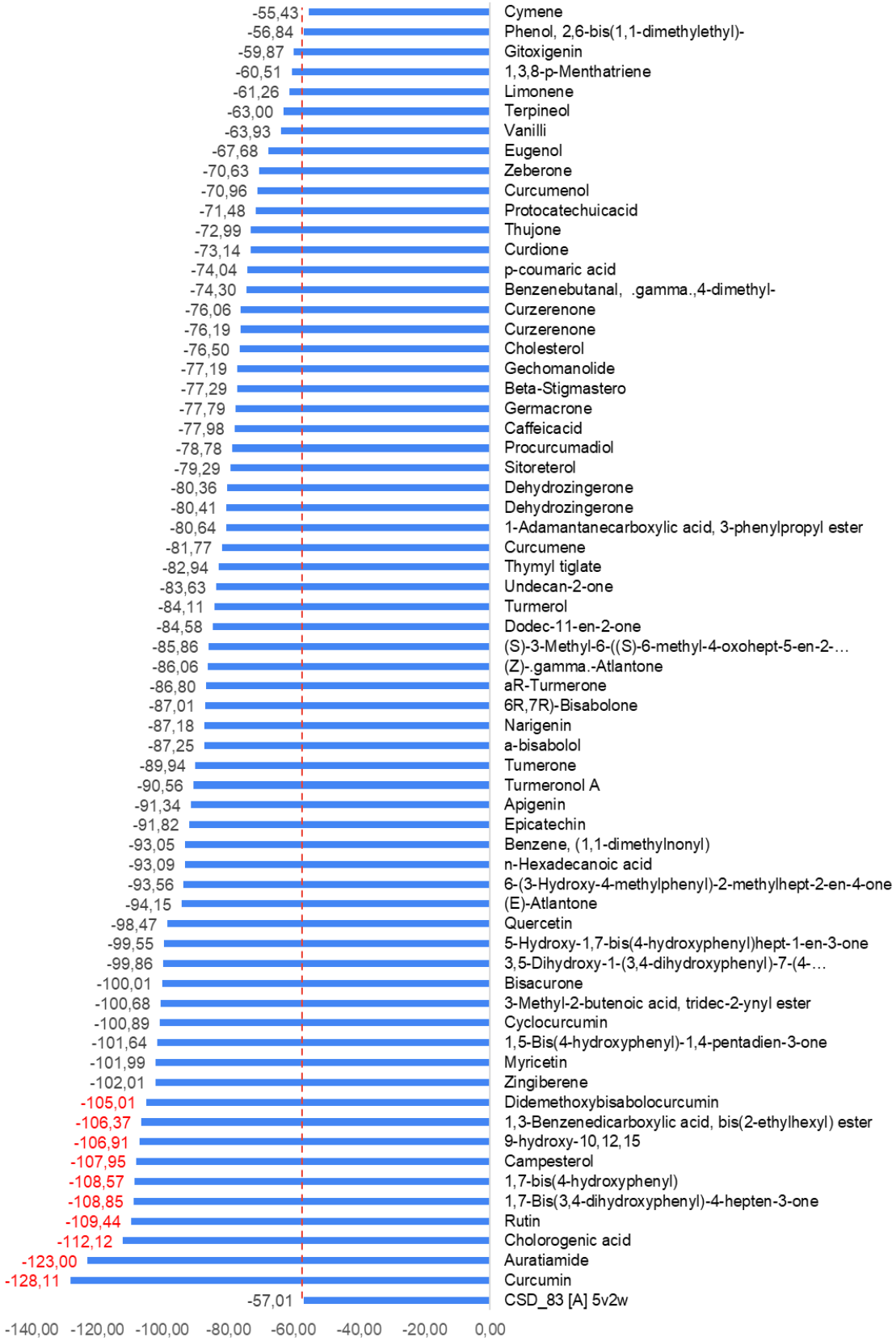

Figure 4. Docking analysis results showing 66 compounds, with 10 top-performing compounds (red letters) based on the rerank score for inhibiting LuxS protein activity

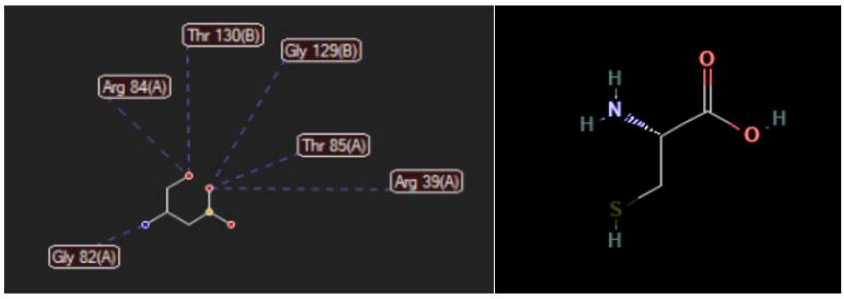

Figure 5. Pharmacophores of the native systeine ligand that interact with the luxS protein are amino groups (-NH2), thiol (-SH), and carboxylate (carbonyl (-C=O) and hydroxyl (-OH))

Tabel 1. Hydrogen bond of ligand

Ligand Names	Hydrogen Bonds
CSD 83[A]	Thr 130, Arg 39, Thr 85, Gly 82, Arg 84, Gly 129
Curcumin	Arg 39, Arg 84, Thr 130, Glu 57
Auratiamide	Arg 39, Arg 84, Thr 130, Thr 85, Cys 41
Cholorogenic acid	Arg 84, Thr 130, Gln 127, His 58, His 54, Gly 129, Met 81, Met 48
Rutin	Arg 84, Thr 130, Glu 57, His 58, His 54, Gly 129, Met 81,Thr 84, Gly 86, Gly 82, Ser 79, Pro 80
1,7-Bis(3,4-dihydroxyphenyl)-4-hepten-3-one	Arg 39, Arg 84, Thr 130, Thr 85, Cys 41
1,7-bis(4-hydroxyphenyl)	His 11, Cys 128, Gln 127, His 54 , Gly 82, Pro 49
Campesterol	Arg 84
9-hydroxy-10,12,15	Thr 130, Cys 128
1,3-Benzenedicarboxylic acid, bis(2-ethylhexyl) ester	Thr 130, Cys 128
Didemethoxybisabolocurcumin	Arg 84, Gly 82

Table 2. Results of lipinski analysis and toxicity

Ligand Name	Molecular Weight	Log P	Hydrogen Donor	Hydrogen Acceptor	Skin Sensitization	AMES Toxicity
CSD 83[A]	121.161	-0.672	3	3	-	-
Curcumin	368.385	3.369	2	6	No	No
Auratiamide	354.311	-0.646	6*	8	No	No
Cholorogenic acid	402.494	2.747	3	3	No	Yes*
Rutin	610.521*	-1.687	10*	16*	No	No
1,7-Bis(3,4-dihydroxyphenyl)-4-hepten-3-one	328.364	3.199	4	5	No	No
1,7-bis(4-hydroxyphenyl)	292,334	3,949	2	3	No	Yes*
Campesterol	400,691	7,635*	1	1	No	No
9-hydroxy-10,12,15	294,435	4,631	2	2	No	Yes*
1,3-Benzenedicarboxylic acid, bis(2-ethylhexyl) ester	390,564	6,433*	0	4	No	No
Didemethoxybisabolocurcumin	542,672*	6,766*	3	6	No	No

Description: * Does not meet the requirements

Based on the predicted molecular properties of the ligands presented in Table 2, evaluation was conducted according to Lipinski's Rule of Five, which stipulates that compounds should have a molecular weight below 500 g/mol, a maximum of 5 hydrogen bond donors, fewer than 10 hydrogen bond acceptors, and a logP value below 5 (Najib,

2024). Most of the ligands complied with these criteria; however, several compounds, including Rutin (MW = 610.521 g/mol; H-donors = 10; H-acceptors = 16), Campesterol (logP = 7.6347), 1,3-Benzene dicarboxylic acid, bis(2-ethylhexyl) ester (logP = 6.433), and Didemethoxybisabolocurcumin (logP = 6.7658), exceeded the recommended thresholds. Elevated molecular weight and high logP values suggest that these compounds may encounter difficulties permeating cell membranes and could exhibit strong membrane binding, potentially limiting their accessibility to target enzymes.

Several compounds exhibited relatively high lipophilicity, which may influence the balance between aqueous solubility and membrane permeability and consequently limit passive diffusion across biological membranes, potentially reducing systemic bioavailability according to Lipinski's Rule of Five. Nevertheless, molecular docking results demonstrated that several ligands maintained favorable binding interactions with the target protein through stable hydrogen bonding and other non-covalent interactions within the active site. These findings suggest that, despite deviations from Lipinski's criteria, the compounds still possess effective molecular recognition toward the biological target. Importantly, such physicochemical characteristics particularly high molecular weight and polarity may limit transdermal penetration and systemic absorption while promoting retention on the skin surface or superficial layers. Consequently, rather than indicating a pharmacokinetic limitation alone, these Lipinski rule violations provide practical insight that the compounds may be more suitable for localized pharmacological activity as topical agents. Further studies, including skin permeation experiments and molecular dynamics simulations, are recommended to better understand ligand–protein interaction stability and the diffusion behavior of these compounds in biologically relevant systems.

Toxicity analysis was performed using the pkCSM platform, focusing on skin sensitization and Ames toxicity parameters. All ligands tested negative for skin sensitization, indicating a low risk of dermal adverse effects. However, the Ames test revealed potential mutagenicity for several compounds, namely chlorogenic acid, 1,7-bis(4-hydroxyphenyl), and 9-hydroxy-10,12,15. The Ames test evaluates a compound's capacity to induce genetic mutations by altering DNA. It is important to note that these results are derived from in silico toxicity prediction models, which provide preliminary risk assessments rather than definitive biological outcomes. Despite

these predictions, empirical evidence regarding turmeric rhizome indicates no observed carcinogenic or mutagenic effects associated with its consumption. Conversely, curcumin, a major bioactive constituent of turmeric, has been widely reported to exhibit significant antimutagenic properties. Curcumin can protect DNA integrity by preventing structural damage, neutralizing free radical activity, and inhibiting the formation of potentially toxic DNA adducts (Najib, 2024). Furthermore, computational Ames toxicity models are known to occasionally produce false-positive predictions for polyphenolic compounds due to their high chemical reactivity and redox activity within simulation frameworks, which may not necessarily reflect their actual biological behavior. Therefore, these predictions should be interpreted cautiously and ideally validated through further experimental toxicological studies.

4. Phytochemical Screening

Phytochemical screening of turmeric extracts and fractions (Table 3) revealed variations compared to the findings reported by Armilda et al. (2022). In contrast to the previous study, tannins were not detected in the present analysis. This difference may be associated with storage conditions that could influence the stability of certain secondary metabolites. In this study, the extract was stored at 0°C in a dark container for approximately one year prior to analysis. Prolonged storage, even under low-temperature and light-protected conditions, may contribute to gradual degradation or structural modification of certain phenolic compounds, including tannins, which could reduce their detectability during qualitative screening. Conversely, saponins were identified in the present study but were not reported in the earlier work, which may be related to differences in sample quantity and the use of an aqueous suspension without additional solvents during the screening procedure. Furthermore, the detection of triterpenoids was facilitated by sample preparation involving chloroform extraction followed by solvent evaporation and the addition of Liebermann–Burchard reagent, enabling clearer visualization of these metabolites.

Table 3. Phytochemical test results

Compound Groups	Extract	Methanol Fraction	Hexane Fraction	Ethyl acetate Fraction	Water Fraction
Saponins	+	-	-	-	+
Alkaloids	-	-	-	-	-
Polyphenols	+	-	-	+	-
Flavonoids	++++	++	-	++++	+
Tannin	-	-	-	-	-
Triterpenoids	++++	++	+	++++	+
Steroids	-	-	-	-	-
Antraquinones	+++	-	-	++++	-

Description: (-) Negative; (+) Positive weak intensity; (++) Positive moderate intensity; (+++) Positive strong intensity, (++++) Positive very strong intensity

5. Total Curcuminoid

Quantitative analysis of curcuminoid content was conducted on the crude extract, ethyl acetate fraction, and methanol fraction (Table 4). The highest concentration was observed in the ethyl acetate fraction (24.88% w/w), followed by the 70% ethanol extract (21.69% w/w), whereas the methanol fraction contained only 0.83% w/w, which is below the minimum requirement of 11.17% established by the *Indonesian Herbal Pharmacopoeia* (2017). These findings are consistent with those of Armilda et al. (2022), which reported a similar rank order of curcuminoid distribution, although with lower absolute values, likely due to differences in analytical methods and storage conditions. The higher standard deviation in the ethyl acetate fraction suggests greater variability in concentration, attributable to its semi-polar nature and sensitivity to storage. The substantial curcuminoid levels in the ethyl acetate fraction and ethanol extract highlight their potential bioactivity and suitability for further development, whereas the methanol fraction is not recommended due to its substandard content. Thus, curcuminoid quantification serves both as a quality control measure and as a scientific basis for selecting fractions or extracts for subsequent pharmacological evaluation, aligning with pharmacopeial principles to ensure consistency, safety, and efficacy of herbal medicines.

Table 4. Total curcuminoid test results

Sample Name	Total Curcuminoid Content (%w/w)	Standard Deviation	Acceptability	Information
Turmeric rhizome extract	21.69	0.09	>11.17	Qualify
Ethyl acetate fraction	24.88	2.4	>11.17	Qualify
Methanol fraction	0.83	0.8	>11.17	Not compliant

6. Antibacterial Activity

The antibacterial assay of turmeric rhizome extract and its fractions (Figure 6) showed that the aqueous fraction exhibited no inhibition zones at any tested concentration, indicating the absence of antibacterial activity against *S. aureus*. This result is consistent with its phytochemical profile, which is dominated by semi-polar metabolites such as flavonoids and polyphenols. These compounds are generally less effective against Gram-positive bacteria due to their limited ability to penetrate the thick peptidoglycan layer, particularly in the absence of lipophilic components. In contrast, the ethyl acetate fraction demonstrated the highest inhibition zone diameter (7.23 mm) at 7.5% concentration, which, according to Davis and Stout (1971), corresponds to moderate antibacterial activity. This activity is supported by its high curcuminoid content (24.88%), as curcuminoids have been reported to inhibit *S. aureus* growth through protein synthesis inhibition, biofilm disruption, and induction of oxidative stress (Zheng et al., 2020).

The ethanol extract exhibited a similar activity pattern to the ethyl acetate fraction, although with slightly lower inhibition at low concentrations. This suggests that the presence of compounds with varying polarity in the crude extract may produce synergistic effects, enhancing antibacterial activity, albeit not as strongly as the more enriched ethyl acetate fraction containing higher levels of active curcuminoids (Ramadhan et al., 2024).

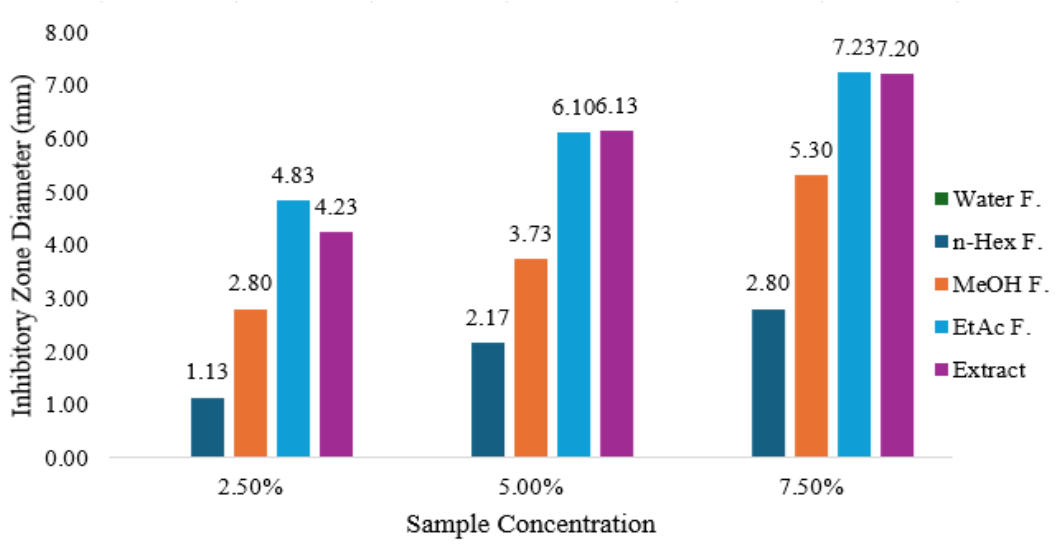

Figure 6. Results of the antibacterial activity test of turmeric rhizome extract and its fractions; the graph shows that the ethyl acetate extract and fraction have dominant activity in the medium category at a concentration of 7.5%.

7. The *S. aureus* Biofilm Formation and Antibiofilm Activity

The biofilm formation assay of *S. aureus* confirmed that incubation at 37 °C for 48 h in BHIB supplemented with 5% glucose represented optimal conditions for biofilm development. This finding is consistent with Holmberg et al. (2009), who demonstrated that glucose-enriched BHIB enhances biofilm formation. In addition to the culture medium, incubation time was also found to be a critical factor; as reported by Sivasankar et al. (2016), a 48 h incubation period is sufficient to establish mature biofilms (Figure 7).

Following the evaluation of antibacterial activity and biofilm-forming ability of *S. aureus*, antibiofilm assays were performed. These preliminary assays were essential to determine the minimum bactericidal concentration and to establish sub-inhibitory concentrations suitable for antibiofilm testing, as viable cells are required to assess the extent of biofilm inhibition. Based on antibacterial results, two samples were selected: the 70% ethanol extract and the ethyl acetate fraction of turmeric rhizomes. Antibiofilm activity was assessed using the crystal violet assay in 48-well microplates.

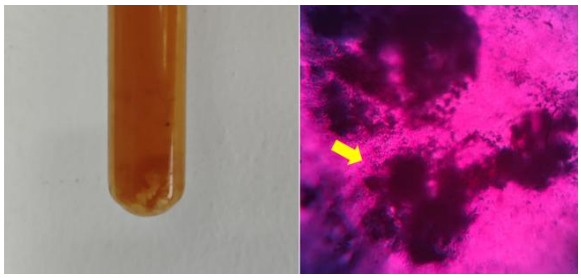

(a) (b)

Figure 7. (a) Biofilm formation of *S. aureus*; (b) Microscopic biofilm formation at 1000× optical magnification and 2× digital magnification, showing (yellow arrow) planktonic *S. aureus* cells emerging from the biofilm.

Viability testing demonstrated that *S. aureus* remained viable at all concentrations of the ethanol extract (Figure 8); however, biofilm formation was inhibited at 0.5–1%, with the minimum biofilm inhibitory concentration (MBIC) established at 0.5%. In contrast, the ethyl acetate fraction exhibited markedly higher potency, with an MBIC of 0.05%, indicating tenfold greater efficacy compared to the crude extract. Quantitative biofilm analysis based on OD_{590} values and IC_{50} calculations further supported this result, showing that the ethyl acetate fraction had an IC_{50} value approximately 20-fold lower than the ethanol extract. These findings demonstrate that the ethyl acetate fraction is

significantly more effective in preventing *S. aureus* biofilm formation, as lower IC_{50} values reflect stronger antibiofilm activity.

Analysis of MBIC and IC_{50} values confirmed that the ethyl acetate fraction exhibited the strongest antibiofilm activity compared to other samples (Figure 9). This result is consistent with its phytochemical profile, as the ethyl acetate fraction contained the highest total curcuminoid content. Curcuminoids, the key phytochemical markers of turmeric rhizomes, have been reported to interfere with biofilm formation through multiple mechanisms. In silico studies indicate that curcumin targets the AI-2 production pathway, thereby disrupting quorum sensing (QS). Experimentally, curcumin has been shown to inhibit early stages of biofilm development by preventing bacterial adhesion to surfaces, reducing extracellular polymeric substance (EPS) production, and impairing QS regulation of biofilm formation and virulence factor expression (Teow et al., 2016). Moreover, curcumin can destabilize established biofilms, thereby enhancing bacterial susceptibility to conventional antibiotics (Packiavathy et al., 2014). These findings strongly support the ethyl acetate fraction as the most promising candidate for further development as a natural antibiofilm agent.

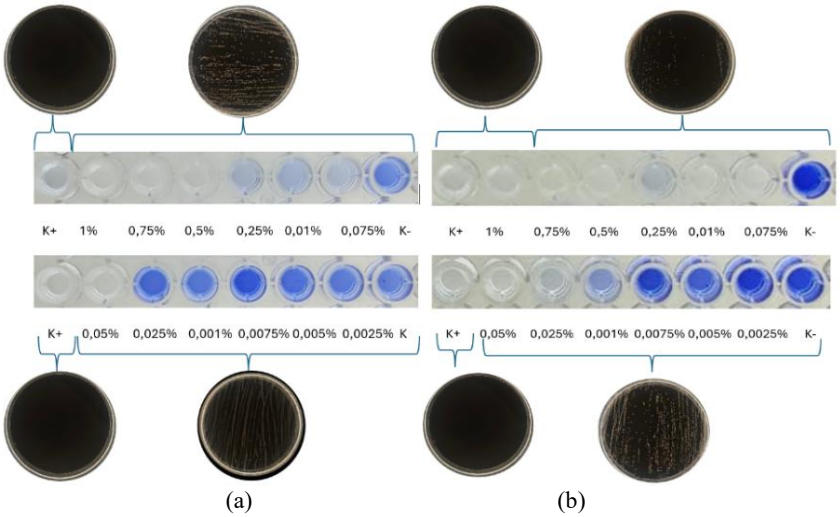

(a) (b)

Figure 8. Staining Results of *S. aureus* Biofilm Using Crystal Violet; the results of staining *S. aureus* biofilm using 0.1% crystal violet show differences in (a) the extract sample with a 0.5% MIC and (b) the ethyl acetate fraction with a 0.05% MIC.

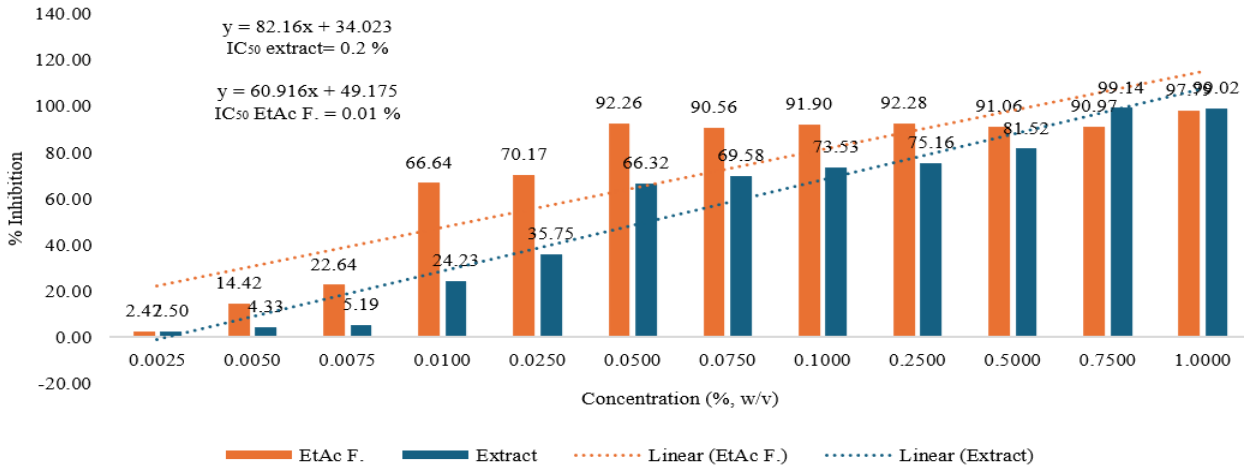

Figure 9. The results of the biofilm formation inhibition test of turmeric rhizome extract IC_{50} = 0.2% and IC_{50} of ethyl acetate (EtAc) fraction = 0.01%; The ethyl acetate fraction has a higher potential compared to the extract

8. Correlation Between In silico and In vitro Results

The integration of in silico and in vitro approaches provides a comprehensive understanding of the antibiofilm potential of turmeric rhizome fractions. Molecular docking analysis identified curcumin, auratiamide, chlorogenic acid, and rutin as top ligands with favorable binding affinities to LuxS (PDB ID: 5V2W), a key enzyme involved in the AI-2 quorum sensing pathway. Curcumin exhibited strong binding interactions within the active site of LuxS and formed interactions with several important residues. Notably, curcumin was predicted to interact with residues such as Arg39 and His58, which have been reported to play critical roles in the catalytic mechanism and substrate stabilization of the LuxS enzyme. The involvement of these residues suggests that curcumin may interfere with the catalytic activity of LuxS, thereby potentially disrupting the synthesis of autoinducer-2 (AI-2) molecules and inhibiting quorum sensing regulation.

These findings are consistent with previous studies reporting that curcumin possesses significant antibiofilm and anti-quorum sensing activities. Curcumin has been shown to inhibit bacterial adhesion, suppress the production of extracellular polymeric substances (EPS), and reduce the expression of quorum sensing-regulated virulence factors. By targeting catalytic residues within LuxS, curcumin may impair AI-2 mediated signaling, which is essential for biofilm maturation and intercellular bacterial communication (Fernandes et al., 2023). Such interference may consequently weaken biofilm formation and pathogenicity in several bacterial species.

Several recent studies support these observations. For instance, curcumin has been reported to interfere with quorum sensing signaling and biofilm development in pathogenic bacteria, including *Pseudomonas aeruginosa* and *S. aureus*, through inhibition of signaling pathways and virulence gene expression (Gholami et al., 2020; Lakhanapuram et al., 2025). Additionally, molecular studies have highlighted that disruption of LuxS-mediated signaling can significantly reduce AI-2 production and biofilm formation, further supporting the potential mechanism predicted in the present docking analysis. Therefore, the docking results obtained in this study provide mechanistic support for the antibiofilm potential of turmeric-derived compounds, particularly curcumin, through possible interference with the LuxS catalytic site.

The strength of this research approach is further reinforced by experimental validation through in vitro assays, allowing direct verification of the computational predictions obtained. The ethyl acetate fraction, characterized by the highest curcuminoid concentration (24.88% w/w), exhibited the strongest antibiofilm activity with a Minimum Biofilm Inhibitory Concentration (MBIC) value of 0.05% and an IC_{50} value approximately 20 times lower than that of the crude ethanol extract. These findings indicate that solvent fractionation effectively enriches active compounds, thereby enhancing their biological potency. In addition, the observed moderate antibacterial activity suggests that curcuminoids not only inhibit biofilm formation but also contribute to bacterial growth suppression, providing a dual effect that is relevant for infection control. The crude ethanol extract demonstrated a similar activity trend but with lower potency, possibly due to the presence of multiple compounds with varying polarities that may interact synergistically, albeit at lower curcuminoid concentrations.

Overall, the combination of computational and experimental approaches represents a key methodological strength of this study, as it enables both the exploration of molecular mechanisms and the empirical verification of biological activity. The strong correlation between docking results and antibiofilm assays indicates that molecular docking is a reliable tool for predicting potential antibiofilm compounds prior to further biological evaluation. This integrative strategy not only improves the efficiency of bioactive compound discovery but also provides a stronger scientific basis for explaining the mechanisms of action of active compounds. Therefore, the

curcuminoid-enriched fraction, particularly the ethyl acetate fraction, can be considered a promising candidate for the development of natural antibiofilm agents against *S. aureus*.

CONCLUSION

In silico analysis revealed that turmeric rhizome (*Curcuma longa*) contains approximately 66 phytochemical compounds, with curcumin identified as the most promising candidate based on rerank scores. Other compounds, including auratiamide, chlorogenic acid, and rutin, also exhibited interaction patterns similar to the native ligand within the biofilm-targeted protein. Consistent with these predictions, in vitro assays demonstrated that the ethyl acetate fraction of turmeric rhizome exhibited higher antibiofilm activity compared to the crude extract. This enhanced activity correlates with the higher total curcuminoid content observed in the ethyl acetate fraction, suggesting its potential as a natural antibiofilm agent against *S. aureus*.

ACKNOWLEDGMENT

We would like to thank Prof. Dr. apt. Siswandono, M.S. for the permission given for the Molegro Virtual Docker application.

CONFLICT OF INTEREST

The authors declare that there are no conflicts of interest associated with this study. The research was conducted independently without any commercial or financial relationships that could be construed as a potential conflict of interest, and the results presented in this manuscript are solely based on scientific considerations.

REFERENCES

Abdullahi, S. H., Moin, A. T., Uzairu, A., Umar, A. B., Ibrahim, M. T., Usman, M. T., Nawal, N., Bayil, I., & Zubair, T. (2024). Molecular docking studies of some benzoxazole and benzothiazole derivatives as VEGFR-2 target inhibitors: In silico design, MD simulation, pharmacokinetics and DFT studies. *Intelligent Pharmacy*, *2*(November 2023), 232–250. https://doi.org/10.1016/j.ipha.2023.11.010

Aji, N., Kumala, S., Mumpuni, E., & Rahmat, D. (2022). Antibacterial Activity and Active Fraction of Zingiber officinale Roscoe , Zingiber montanum (J . Koenig) Link ex A ., and Zingiber zerumbet (L .) Roscoe ex Sm . Against Propionibacterium acnes. *Pharmacon*, *14*(1), 103–111. https://doi.org/10.5530/pj.2022.14.15

Anindyaguna, A., Taolin, A., & Suharmanto. (2025). Faktor yang Berhubungan dengan Acne vulgaris : Literatur Review. *Jurnal Penelitian Perawat Profesional*, *7*(3), 783–790. https://doi.org/https://doi.org/10.37287/jppp.v7i3.6788

Armilda, L. H. V, Puspitasari, A., Indriyana, M., Nuraini, T., & Aji, N. (2022). Antibiofilm Determination Of Curcuma longa L. Rhizome As Drug Candidates In Handling Propionibacterium acnes Resistance. *International Conference on Medical Laboratory Technology*, *2*, 92–105.

Besan, E. J., Rahmawati, I., & Saptarini, O. (2023). Antibiofilm Activity of Butterfly Pea Flower (Clitoria ternatea L.) Extract and Fractions against Staphylococcus aureus. *PHARMACY: Jurnal Farmasi Indonesia (Pharmaceutical Journal of Indonesia)*. https://doi.org/https://doi.org/10.30595/pharmacy.v0i0.14437

Chen, L., Wilksch, J. J., Liu, H., Zhang, X., Torres, V. V. L., Bi, W., & Mandela, E. (2020). Investigation of LuxS- -mediated quorum sensing in Klebsiella pneumoniae. *Journal of Medical Microbiology*, *69*, 402–413. https://doi.org/10.1099/jmm.0.001148

Davis, W. W., & Stout, T. R. (1971). Disc plate method of microbiological antibiotic assay. I. Factors influencing variability and error. *Applied Microbiology*, *22*(4), 659–665. https://doi.org/10.1128/am.22.4.659-665.1971

Farnsworth, N. R. (1966). Biological and Phytochemical Screening of Plants. *Journal of pharmaceutical sciences*, *55*(3), 225–276. https://doi.org/https://doi.org/10.1002/jps.2600550302

Fernandes, S., Borges, A., Gomes, I. B., Sousa, S. F., & Simoes, M. (2023). Curcumin and 10-undecenoic acid as natural quorum sensing inhibitors of LuxS/AI-2 of Bacillus subtilis and LasI/LasR of Pseudomonas aeruginosa. *Food Research International*, *165*(January), 1–10. https://doi.org/10.1016/j.foodres.2023.112519

Gehrke, A. K. E., Giai, C., & Gómez, M. I. (2023). Staphylococcus aureus Adaptation to the Skin in Health and Persistent/Recurrent Infections. *Antibiotics*, *12*(10), 1–26. https://doi.org/10.3390/antibiotics12101520

Gholami, M., Zeighami, H., Bikas, R., Heidari, A., Rafiee, F., & Haghi, F.

(2020). Inhibitory activity of metal - curcumin complexes on quorum sensing related virulence factors of Pseudomonas aeruginosa PAO1. *AMB Express*, *10*(11), 1–10. https://doi.org/10.1186/s13568-020-01045-z

Hanifitri, A., Ambarsari, L., & Mubarik, N. R. (2023). Pemodelan protein dan analisis molecular docking enzim β-glukanase solat Bacillus subtilis W3.15. *E-Journal Menara Perkebunan*, *91*(1), 59–71. https://doi.org/10.22302/iribb.jur.mp.v91i1.523

Heng, A. H. S., & Chew, F. T. (2020). Systematic review of the epidemiology of acne vulgaris. *Scientific Reports*, *10*(1), 1–29. https://doi.org/10.1038/s41598-020-62715-3

Holmberg, A., Lood, R., Mörgelin, M., Söderquist, B., Holst, E., Collin, M., Christensson, B., & Rasmussen, M. (2009). Biofilm formation by Propionibacterium acnes is a characteristic of invasive isolates. *Clinical Microbiology and Infection*, *15*(8), 787–795. https://doi.org/https://doi.org/10.1111/j.1469-0691.2009.02747.x

Ibrahim, Y. M., Abouwarda, A. M., & Omar, F. A. (2020). Effect of kitasamycin and nitrofurantoin at subinhibitory concentrations on quorum sensing regulated traits of Chromobacterium violaceum. *Antonie van Leeuwenhoek*, *113*(11), 1601–1615. https://doi.org/https://doi.org/10.1007/s10482-020-01467-6

Kashi, M., Noei, M., Chegini, Z., & Shariati, A. (2024). Natural compounds in the fight against Staphylococcus aureus biofilms: a review of antibiofilm strategies. *Frontiers in Pharmacology*, *15*(November), 1–25. https://doi.org/10.3389/fphar.2024.1491363

Kemenkes RI. (2008). *Farmakope Herbal Indonesia*. Kementerian Kesehatan RI.

Kemenkes RI. (2017). *Farmakope Herbal Indonesia* (II). Kementerian Kesehatan RI.

Lakhanapuram, H. K., Bunluepuech, K., Somsiripan, T., Khongkhai, H., Sangkanu, S., Saengsawang, P., Nissapatorn, V., & Pereira, M. de L. (2025). Assessment of antibacterial , antibiofilm, and physicochemical characteristics of Curcuma longa L . extract and soap containing C . longa extract against Staphylococcus aureus. *Journal of the Saudi Society of Agricultural Sciences*, *24*(65), 1–18.

https://doi.org/https://doi.org/10.1007/s44447-025-00066-z

Legiawati, L., Halim, P. A., Fitriani, M., Hikmahrachim, H. G., & Lim, H. W. (2023). Microbiomes in Acne Vulgaris and Their Susceptibility to Antibiotics in Indonesia: A Systematic Review and Meta-Analysis. *Antibiotics*, *12*(1), 1–17. https://doi.org/10.3390/antibiotics12010145

Najib, A. (2024). Studi In Silico Prediksi Sifat Fisikokimia dan Toksisitas Senyawa Tectoquinone Sebagai $α$-Glukosidase inhibitor. *Makassar Natural Product Journal (MNPJ)*, *2*(3), 215–221. https://doi.org/10.33096/mnpj.v2i3.217

Navidifar, T., Zare Banadkouki, A., Parvizi, E., Mofid, M., Golab, N., Beig, M., & Sholeh, M. (2025). Global prevalence of macrolide-resistant Staphylococcus spp.: a comprehensive systematic review and meta-analysis. *Frontiers in Microbiology*, *16*(March). https://doi.org/10.3389/fmicb.2025.1524452

Packiavathy, I. A. S. V., Priya, S., Pandian, S. K., & Ravi, A. V. (2014). Inhibition of biofilm development of uropathogens by curcumin–an anti-quorum sensing agent from Curcuma longa. *Food chemistry*, *148*, 453–460. https://doi.org/https://doi.org/10.1016/j.foodchem.2012.08.002

Ramadhan, M. F., Supriani, Sari, W. Y., Khotimah, K., & Setyaningsih, M. (2024). Uji Fitokimia Ekstrak Etanol 96% dan Fraksi Air, Fraksi Klorofom serta Fraksi n-Hexana Rimpang Kunyit (Curcuma Longa L.). *Jurnal Farmasetis Volume*, *13*(2), 71–78. https://doi.org/https://doi.org/10.32583/far.v13i2.2258

Reynolds, R. V., Yeung, H., Cheng, C. E., Cook-Bolden, F., Desai, S. R., Druby, K. M., Freeman, E. E., Keri, J. E., Stein Gold, L. F., Tan, J. K. L. L., Tollefson, M. M., Weiss, J. S., Wu, P. A., Zaenglein, A. L., Han, J. M., & Barbieri, J. S. (2024). Guidelines of care for the management of acne vulgaris. *Journal of the American Academy of Dermatology*, *90*(5), 1006.e1-1006.e30. https://doi.org/10.1016/j.jaad.2023.12.017

Sivasankar, C., Maruthupandiyan, S., Balamurugan, K., James, P. B., Krishnan, V., & Pandian, S. K. (2016). A combination of ellagic acid and tetracycline inhibits biofilm formation and the associated virulence of

Propionibacterium acnes in vitro and in vivo. *Biofouling*, *32*(4), 397–410. https://doi.org/https://doi.org/10.1080/08927014.2016.1148141

Teow, S.-Y., Liew, K., Ali, S. A., Khoo, A. S.-B., & Peh, S.-C. (2016). Antibacterial action of curcumin against Staphylococcus aureus: a brief review. *Journal of tropical medicine*, *2016*(1), 2853045. https://doi.org/https://doi.org/10.1155/2016/2853045

Warren, G. L., Andrews, C. W., Capelli, A.-M., Clarke, B., LaLonde, J., Lambert, M. H., Lindvall, M., Nevins, N., Semus, S. F., & Senger, S. (2006). A critical assessment of docking programs and scoring functions. *Journal of medicinal chemistry*, *49*(20), 5912–5931. https://doi.org/https://doi.org/10.1021/jm050362n

Winato, B. M., Sanjaya, E., Siregar, L., Kifami, S., Maria, Y., Fau, V., & Mutia, M. S. (2019). Acnes Antibacterial Activity Of Serai Wangi Leaf Extract (Cymbopogon nardus) Against Propionibacterium acnes. *Jurnal Biologi Lingkungan*, *6*(1). https://doi.org/10.31289/biolink.v6i1.2210

Zheng, D., Huang, C., Huang, H., Zhao, Y., Khan, M. R. U., Zhao, H., & Huang, L. (2020). Antibacterial Mechanism of Curcumin: A Review. *Chemistry and Biodiversity*, *17*(8). https://doi.org/10.1002/cbdv.202000171